

Transmission Characteristics of 1D Metallo-dielectric Photonic Crystal with a Defect Rod

T.P. Negara^{1, #}, Mardanih^{2, 3}, H. Hardhienata³, and H. Alatas³

¹⁾Computer Science Department, Pakuan University, Jl. Pakuan, Bogor 16143, Indonesia

²⁾Graduate School of Biophysics, Bogor Agricultural University, Bogor 16680, Indonesia

³⁾Theoretical Physics Division, Departement of Physics, Bogor Agricultural University, Kampus IPB Darmaga, Bogor 16680, Indonesia

teguhpujanegara@yahoo.com

Abstract. In this paper we report the transmission characteristics of a 1D metallo-dielectric photonic crystal with a defect rod located in the middle of the structure. Simulations of the field propagation for the corresponding TE and TM modes were carried out using Finite Difference Time Domain (FDTD) technique on Maxwell's Equation. The results show that for certain chosen parameters of the structure the field energy varies if the refractive index of the defect rod is changed and that approximate linier changes in time average energy density W exists for an refractive index range of 1.3 – 1.5 with a slight increase for TM case and a relatively steep decrease for TE case. The characteristics change due to variation of the defect rod radius is also considered.

Keywords: FDTD method, Optical Biosensor, One-Dimensional Photonic Crystal

PACS: 42.82.Et, 41.20.Jb, 42.70.Qs

INTRODUCTION

Photonic Crystal (PhC) concepts have triggered interest in the investigation of electromagnetic wave propagation in photonic ban-gap structures. Many numerical simulation methods have been developed to understand the principles of various different PhC structures to develop devices with specific functions [1]. The unique nature of PhC's promises, among other applied fields, many new applications in biosensor [2].

Several methods have been developed previously to solve Maxwell's equation in discretized [3] form. One of the most reliable schemes is the Finite Difference Time Domain (FDTD) [4] with Perfectly Matched Layer [5] for the corresponding boundary condition. The FDTD algorithm to solve Maxwell's equation was first proposed by Yee [4] and since then has been refined by many researchers and becomes one of the most widely used schemes in the studies of PhC.

It has been shown in [6] that a one-dimensional (1D) PhC imbedded by a defect layer inherits a photonic pass-band whose characteristics depend on the change in the material properties of the defect. In this report, we consider the characteristics of a 1D PhC structure consisting of eleven alternating dielectric and metallic rods, with the dielectric rods at the middle is

considered as a defect. It is well known for TE polarizations that the coupling between the free electrons in the metal and the electric wave generates surface plasmons [7]. We found that the transmission of the electric field is affected significantly by the presence of surface plasmons and that the sensitivity of the device alters if the refractive index of the defect rod is varied. For the sake of comparison, we also discuss the TM case.

FDTD FORMULATION

Light propagation inside a photonic crystal material can be described quantitatively by the four Maxwell's equations. For the case of a TE wave where the electric field, $\vec{E}(x, y)$ lies in the $x - y$ plane and the magnetic field $\vec{H}(x, y)$ lies in the z plane, the Maxwell's equations are given as follows:

$$\frac{\partial H_z}{\partial t} = \frac{1}{\sqrt{\epsilon_0 \mu_0}} \left(\frac{\partial E_x}{\partial y} - \frac{\partial E_y}{\partial x} \right) \quad (1)$$

$$\frac{\partial D_x}{\partial t} = \frac{1}{\sqrt{\epsilon_0 \mu_0}} \frac{\partial H_z}{\partial y} \quad (2)$$

$$\frac{\partial D_y}{\partial t} = -\frac{1}{\sqrt{\epsilon_0 \mu_0}} \frac{\partial H_z}{\partial x} \quad (3)$$

along with the relation $D_x = \epsilon_0 \epsilon_r E_x$, $D_y = \epsilon_0 \epsilon_r E_y$.

For the TM case where $\vec{H}(x, y)$ lies in the $x-y$ plane and $\vec{E}(x, y)$ is parallel to the z -axis the Maxwell's equations are given by:

$$\frac{\partial D_z}{\partial t} = \frac{1}{\sqrt{\epsilon_0 \mu_0}} \left(\frac{\partial H_y}{\partial x} - \frac{\partial H_x}{\partial y} \right) \quad (4)$$

$$\frac{\partial H_x}{\partial t} = -\frac{1}{\sqrt{\epsilon_0 \mu_0}} \frac{\partial D_z}{\partial y} \quad (5)$$

$$\frac{\partial H_y}{\partial t} = \frac{1}{\sqrt{\epsilon_0 \mu_0}} \frac{\partial D_z}{\partial x} \quad (6)$$

As stated previously, these Maxwell equations can be solved numerically using the FDTD method and Yee algorithm with PML boundary condition with the detailed formulation given in [4].

To investigate the change in the electric field due to material changes in the defect rod, we consider the amount of energy at the end of the device as a function of time, defined by:

$$Q(t) = \int_0^h \epsilon |\vec{E}(t)|^2 dy \quad (7)$$

with \vec{E} denoting the TE/TM case of the electric field at the left end of the slab and h is the slab thickness. Further, we define the following parameter for a given refractive index of defect rod:

$$W = \frac{1}{t} \int_{t_0}^t Q(t) dt \quad (8)$$

which describes the time average energy density, where t is the corresponding measurement time.

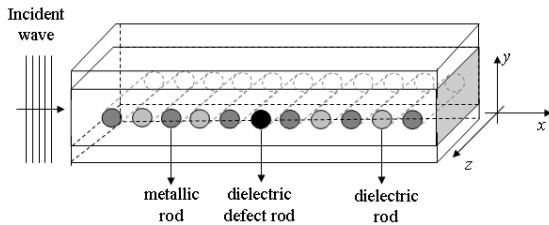
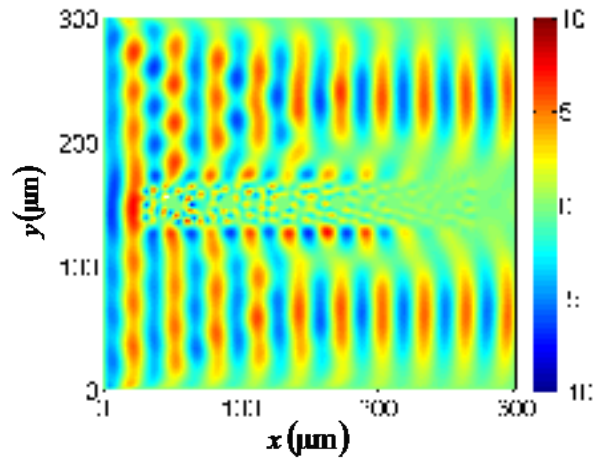


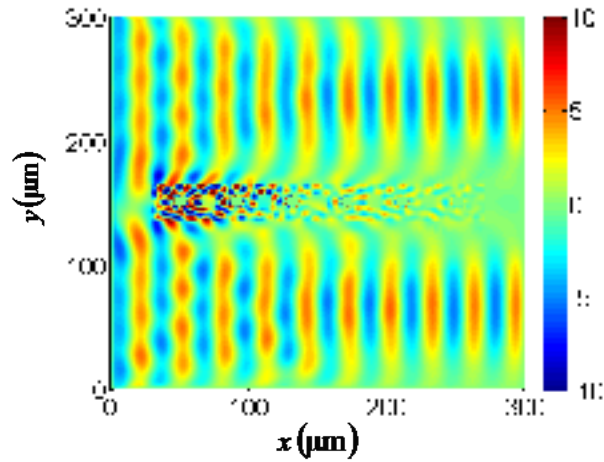
FIGURE 1. Sketch of 1D Metallodielectric Photonic Crystal with defect rod

1D METALLODIELECTRIC PHOTONIC CRYSTAL

The sketch of the model is shown in Fig. 1 which is homogeneous in the z -direction. It is important to note that because the periodicity of the system is only in one dimension, the model is called 1D PhC. For the numerical simulation we use eleven periodic rods for the dielectric material namely silicon (Si) with relative permittivity of $\epsilon_r = 12.11$ and relative permeability of $\mu_r = 1$. For the metallic rod, we choose silver (Ag) with a relative permittivity $\epsilon_r = -18.36 + i4.38$ at 700 nm based on the Brendel-Borman model [8], and a relative permeability $\mu_r = 0.99998$.



(a)



(b)

FIGURE 2. (Color) Snapshot of the real part of electric fields of (a) TM and (b) TE polarizations

The metallic and dielectric rods were inserted in a silicon nitride slab ($n = 1.98$) with additional insertion of a defect rod in the middle of the periodic structure. The incident wave is propagating from the right side of the structure and is measured on the left end. The length of the device is $L = 240 \mu\text{m}$ (ranging from $x = 30 \mu\text{m}$ to $x = 270 \mu\text{m}$) and the total thickness of the device is $h = 30 \mu\text{m}$ (ranging from $y = 135 \mu\text{m}$ to $y = 165 \mu\text{m}$). The device consists of two SiO_2 ($n = 1.98$) rods, each with a radius of $5 \mu\text{m}$ and is sandwiched by one Si ($n = 3.48$) rod having a radius of $20 \mu\text{m}$.

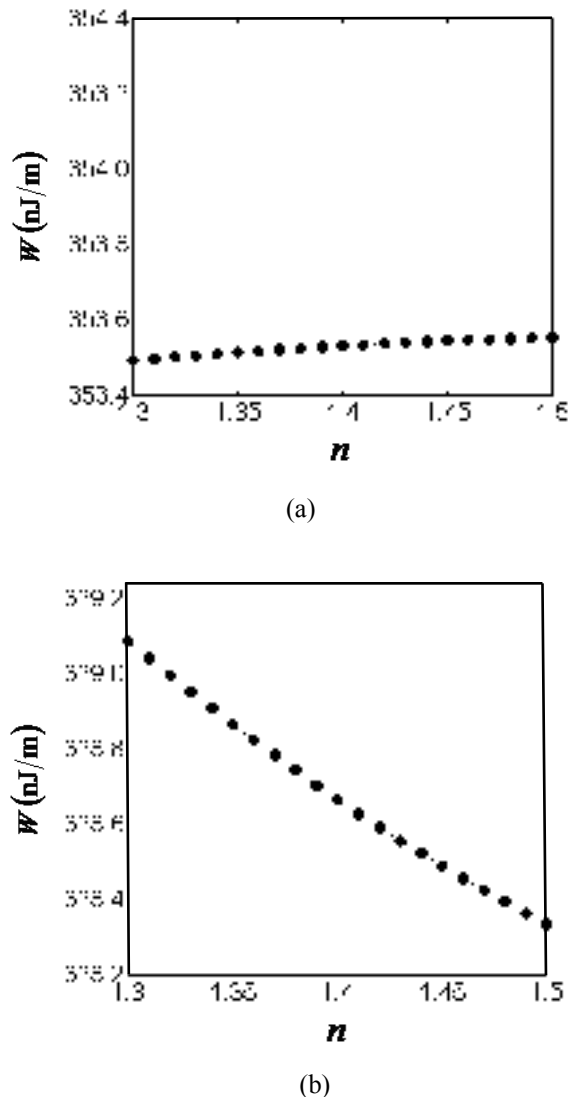


FIGURE 3. The time average energy density W as function of refractive index of defect rod for (a) TM and (b) TE polarizations

RESULT AND DISCUSSION

In our simulation we use a mesh number of 300×300 . Each mesh has a size of $\Delta x = \Delta y = 1 \mu\text{m}$, while the time step is taken to be $\Delta t = 20 \text{ ns}$. The simulation results of the TE and TM polarizations showed interesting significantly different results as is evident from Fig. 2. Fig. 2(a) depicts the snapshot of the real part of the field profiles for TM case, taken at $t = 6 \mu\text{s}$, with the corresponding defect rod having a refractive index of $n = 1.4$ and rod radius of $r = 5 \mu\text{m}$. It is clearly seen that the incoming plane-wave is decaying considerably after colliding with the first two rods due to irregularities caused by the defect material in the middle of the structure and almost vanishes at the last quarter length of the structure. It should be pointed out that the asymmetric field profile with respect to the y -axis arises due to computational limitation in obtaining perfectly circular rods.

Meanwhile, TE propagation in Fig. 2(b) for the same defect, in contrast, shows a relatively slower field decay and higher field around the metallic rod, which is probably caused by the presence of plasmonics at the surface of the silver rod.

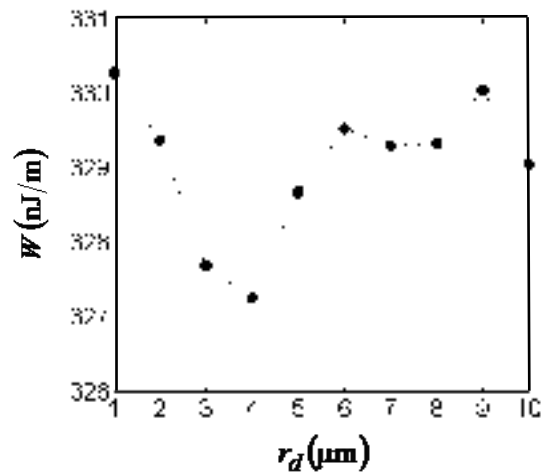


FIGURE 4. The time average energy density W with respect to defect rod radius for TE polarization

The result of field change at the output due to variation in the defect rod refractive index is presented in Fig. 3. For TM wave there is a slight linear like increase in the time average energy density W , defined

by Eq. 7 with $t = 6 \mu\text{s}$, for an refractive index change from 1.3 – 1.5 which is typical for aqueous.

From our numerical calculation, we found that the TE case produces a steeper and decreasing W value for the given defect refractive index interval i.e. from 1.3 to 1.5. In this case the W value is more sensitive to refractive index change in the material. For sensing application a steeper and linier profile is usually more desirable, however this is not always the case as wider interval ranges with lesser linearity are sometimes preferred.

In addition to the above characteristics, we have also calculated the effect of defect rod radius variation (r_d) with respect to W as presented in Fig. 4 for the TE case and reveal that this variation leads to non-monotonous response characteristic. It is easy to see that the highest time average density occur at $r_d = 1 \mu\text{m}$.

CONCLUSION

We have demonstrated by means of FDTD method that an incoming TE and TM plane-wave passing through a 1D metallodielectric photonic crystal with a defect rod can potentially be utilized to build a refractive index sensor due to the existence of linier like relationship between the time average energy W and refractive index change in the defect rod. The linier change varies between the modes with a lower increase of W is obtained for the TE case and steeper decrease is obtained for TM case polarizations. For the TE case, the variation of defect rod radius exhibits a non-monotonous response on the time average energy density.

REFERENCES

1. W. C. L. Hopman, P. Pottier, D. Yudistira, J. Van Lith, P. V. Lambeck, R. M. De La Rue, A. Driessen, H. J. W. M. Hoekstra, and R. M. de Ridder, *IEEE J. Select. Top. Quant. Electron.* **11**, 11-16 (2005)
2. I. D. Block, L. L. Chan, and B. T. Cunningham, *Sensor Act.* **B20** 187-193 (2006)
3. I. A. Sukhoivanov and I. V. Guryev, *Photonic crystal: Physics and Practical Modeling*. New York: Springer, 2009, pp. 103.
4. K. Yee, *IEEE Trans. on Antennas and Propagation*, **14** 302–307 (1966).
5. P. Bérenger, *Perfectly Matched Layer (PML) for Computational Electromagnetics*, Arcueil: Morgan & Claypool Publisher, 2007. pp. 1 - 10
6. H. Alatas, H. Mayditia, H. Hardhienata, A. Iskandar, M. O. Tjia, *Jpn. J. Appl. Phys.* **45**, 6754-658 (2006).
7. G. Acuna, S. F. Heucke, F. Kuchler, H. T. Chen, A. J. Taylor, R. Kersting, *Opt. Expr.* **16**, 18745-18751 (2008)

8. A. D. Rakic, A. B. Djuricic, J. M. Elazar, M. L. Majewski, *Appl. Opt.* **37**, 5271-5283 (1998)